

The Copenhagen problem with a quasi-homogeneous potential

D.Gn. Fakis and T.J. Kalvouridis
 Department of Mechanics, NTUA, Greece

Abstract: We study the Copenhagen case of the RTBP by considering Manev-type quasi-homogeneous potentials.

1 The equations of motion and the zero-velocity curves (zvc) and surfaces (zvs) for the planar motion

The dimensionless equations of motion, in a synodic Cartesian coordinate system $Oxyz$ (Fig.1), with $\omega = 1$, are:

$$\ddot{x} - 2\dot{y} = \frac{\partial U}{\partial x} = U_x, \quad \ddot{y} + 2\dot{x} = \frac{\partial U}{\partial y} = U_y, \quad \ddot{z} = \frac{\partial U}{\partial z} = U_z \quad (1)$$

$$U(x, y, z) = \frac{1}{2} (x^2 + y^2) + \frac{1}{\Delta} \left[\sum_{i=1}^2 \left(\frac{1}{r_i} + \frac{e}{r_i^2} \right) \right] \quad (2)$$

where e is Manev parameter, $r_1 = [(x - 0.5)^2 + y^2 + z^2]^{1/2}$, $r_2 = [(x + 0.5)^2 + y^2 + z^2]^{1/2}$, and $\Delta = 2(1 + 2e) > 0$.

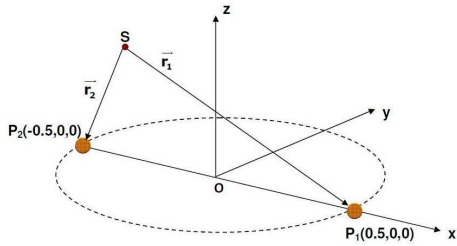


Figure 1

The last condition is satisfied when $e > -0.5$. There is a Jacobian-type integral of motion $\dot{x}^2 + \dot{y}^2 + \dot{z}^2 = 2U(x, y, z) - C$ where C is a constant. When $e < 0$, a “folding” of the chimney-like zvs $C = C(x, y)$ around each primary, starts to form. As a consequence, a closed area of non permitted motion in the vicinity of each primary is created (Fig.2).



Figure 2: The $C = C(x, y)$ surface (left) and the detail of its “folding” (right) for $e = -0.08$

2 Focal curves and equilibrium positions

We use the term “focal curve” to denote the existing common intersection curve of all $C = C(x, y)$ surfaces drawn for various values of e . This curve is shown in Fig.3(b).

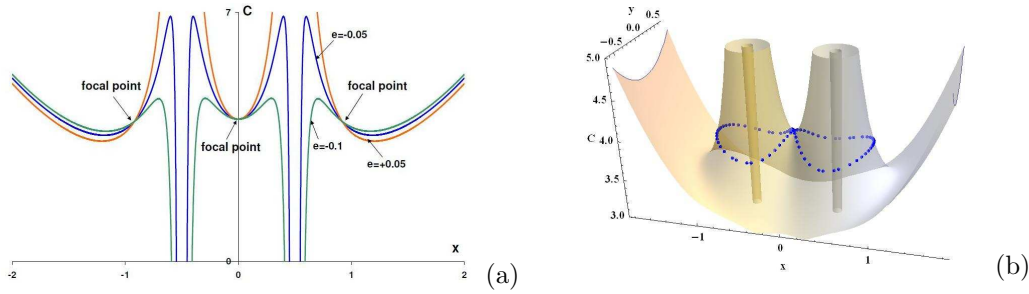


Figure 3: (a) Diagrams xC for various values of e and $y = 0$ and the focal points, (b) the 3d focal curve as it evolves around zero-velocity surface in xyC space

Regarding the equilibrium points, when $e > 0$, the existing equilibria are the same as in the gravitational case. However, when $-0.5 < e < 0$, new equilibria appear (Fig.4). In Table 1 we give the data assigned to these points.

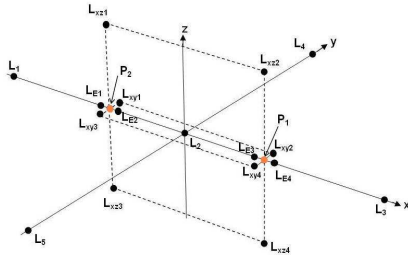


Figure 4: Distribution of the existing equilibria for $e > -0.23$

Table 1

Equilibria	Axis or Plane	Number of Equilibria	Range of e	Stability
L_1, L_3	x-axis	2	$e > -0.1955$	Unstable
L_2	x-axis	1	$e > -0.5$	Unstable
L_4, L_5	x-axis	2	$e > -0.5$	Unstable
E_1, E_4	x-axis	2	$-0.1955 < e < 0$	Unstable
E_2, E_3	x-axis	2	$-0.1820 < e < 0$	Unstable
L_{xy}	xy-plane	4	$-0.5 < e < 0$	Unstable
L_{xz}	xz-plane	4	$-0.5 < e < 0$	Unstable
L_y	y-axis	2	$-0.5 < e < -0.23$	Unstable
L_{+z}, L_{-z}	z-axis	2	$-0.5 < e < -0.25$	Unstable

3 Zero velocity surfaces (zvs) for the 3D motion

In Fig.5 we depict some phases of the evolution of the zvs when $C \geq C_{Lxz}$. We note that bifurcations in the topology of the zvs occur when $C = C_j$, where C_j is the Jacobian of an existing equilibrium.

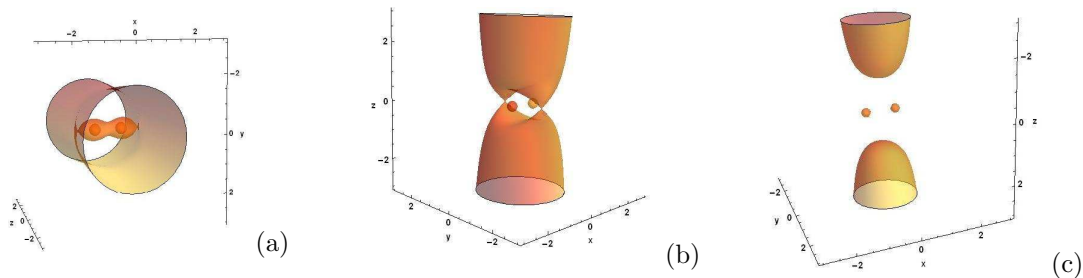


Figure 5: The zvs for $e = -0.14$ and: (a) $C = 3.769$, (b) $C = 3.138$, (c) $C = 2$

References

- [1] Fakis, D.Gn., Kalvouridis, T.J.: *Dynamics of a small body in a Maxwell ring-type N-body system with a spheroid central body*. Cel. Mech.Dyn.Astron. 116 (2013) No 3, 229-240.
- [2] Fakis, D.Gn.: *Numerical investigation of the dynamics of a small body in a Maxwell ring-type N-body system where the central primary creates a Manev-type post-Newtonian potential field*. Doctoral Thesis, 2014, pp.1-667, NTUA.